Available online at www.sciencedirect.com
ScienceDirect
Applied Catalysis A: General 321 (2007) 7–16
APPLIED CATALYSIS A: GENERAL
www.elsevier.com/locate/apcata

Effect of the location of cobalt species on NO adsorption and NO_x-SCR over Co–mordenite

Laura B. Gutierrez *, Eduardo E. Miró, María A. Ulla

Instituto de Investigaciones en Catálisis y Petroquímica, INCAPE (FIQ, UNL-CONICET), Santiago del Estero 2829, 3000 Santa Fe, Argentina

Received 27 October 2006; received in revised form 20 December 2006; accepted 27 December 2006
Available online 18 January 2007

Abstract

A thorough characterization of Co–mordenite was carried out using NO-TPD, H_2-TPR, Raman, DRX and FTIR with NO as probe molecule. Different cobalt-loading catalysts (8.85, 5.70, 2.91, 2.45 and 1.15 wt.%) were prepared by ion exchange over NH_4–mordenite and treated with different procedures (heated on He, O_2 and H_2). The effect of adding water to the reaction stream at 500 °C on the location of the cobalt species was also analyzed. All catalysts were evaluated for the SCR of NO_x with methane as a test reaction both under dry and wet conditions. The NO adsorption capacity depended not only on the Co/Al ratio and pretreatments but also on the presence of Co oxides. In fact, for similar Co/Al ratios, $Co_{2.91}$MOR showed a lower NO/Co ratio than $Co_{2.45}$MOR due to the higher Co_3O_4 concentration in the former. These species probably blocked the main mordenite channels and/or produced the formation of some Co island on the zeolite surface, lowering the amount of surface Co. The main NO surface species detected were dinitrosyl and mononitrosyl. Their stability and relative amount depended on the cobalt species and the pretreatments. Heating in He or H_2 induced the stabilization of part of the exchanged Co in less gas-accessible sites, whereas the calcination with O_2 involved the mobilization of Co to more external sites. However, those effects were less significant for samples containing Co oxides suggesting that the spinel hinders the Co migration. During the wet reaction treatment, the cobalt mobilization to hidden positions occurred along with the formation of Co-oxides, which negatively affected both the catalytic activity and the NO adsorption capacity.

Keywords: NO-TPD; Co–NO interaction; Co–mordenite; Co species on the SCR

1. Introduction

Two decades ago, Li and Armor [1–3] demonstrated that Co–zeolites catalyze the selective reduction of NO with methane in oxygen excess. Since then, several authors have investigated the nature of the cobalt species inside the ion-exchanged Co–zeolites which constitute a promising system for the abatement of NO_x from exhaust gases mainly produced by combustion processes [1–6]. The results of this bulk of research indicate that activity and selectivity depend on several catalyst features such as zeolite topology, Si/Al ratio, acidity, type of cobalt species present in the zeolitic matrix, their interaction with the structure, cobalt coordination to the framework and the distances between the Co ions. The main cobalt species which contribute to the catalyst performance are cobalt oxides, cobalt cations located in the inner zeolite volume (exchanged Co^{2+}), and highly dispersed polynuclear oxo-Co, among others. On the other hand, the concentration of Co is not linearly proportional to the catalytic activity of the Co–zeolite [1–3,5,7], indicating that the location and coordination of Co^{2+} at different cationic sites might play an important role in the catalytic activity. The results reported by Kaucký et al. [5] follow the same trend. They analyzed the Co sites by UV–vis–NIR and IR experiments and compared their activities and selectivities over different zeolitic structures: MFI, FER and MOR. They found that the most active Co sites in ferrierite and mordenite are α-type Co ions and β-type in Co-MFI. Besides, the effect of topology of the zeolite Co ions is dramatic on the CH_4-SCR catalytic activity [5,7,8]. Gutierrez et al. reported [4] that the treatment of CoNa–MOR with hydrogen negatively affects the NO to N_2 conversion for the SCR of NO with CH_4, indicating that the pretreatment has some influence also on the cobalt topology.

* Corresponding author. Tel.: +54 342 4536861; fax: +54 342 4536861.
E-mail address: lbgutier@fiqus.unl.edu.ar (L.B. Gutierrez).

0926-860X/$ – see front matter © 2007 Elsevier B.V. All rights reserved.
doi:10.1016/j.apcata.2006.12.022

It has been reported that cobalt ions can migrate to different positions during calcination pretreatment or during time-on-stream under typical SCR conditions. In their new location, the coordination with the zeolite matrix can change [9,10–12].

The aim of this work is to study the effect of different pretreatments together with the metal content on the types of cobalt species present in the zeolitic matrix. It also analyzes the contribution of these species to the NO adsorption capacity and the catalytic performance for the SCR of NO_x with methane in O_2 excess. The treatments were: (a) heating with different gas flow (O_2, H_2 or He) and (b) adding water (2%) to the reaction stream (wet reaction mixture) in which the catalysts were under reaction stream at 500 °C for 10 h.

2. Experimental

2.1. Catalyst preparation

The catalysts were prepared by ion exchange starting from Na–mordenite (Na–MOR) manufactured by Zeolyst International (Product ID: CBV 10A; Lot. No. 1822-50, Si/Al = 6.5). The ion-exchanged forms, Mordenite (NH_4–MOR) and Co, NH_4–mordenite, were prepared following the procedure described in Gutierrez et al. [4]. Briefly, NH_4–MOR was obtained using a solution of NH_4NO_3 keeping it on reflux at 100 °C for 24 h. An aliquot of NH_4–MOR was exchanged with a solution of $Co(CH_3COO)_2$ to produce Co_xMOR (x = 8.85, 5.70, 2.91, 2.45 and 1.15 wt.% Co). In order to obtain different degrees of cobalt concentration exchange, the exchange time was modified. After the exchange, the solids were filtered, washed, and dried. Co_xMOR was treated following different procedures: (a) heating up to 500 °C in O_2 flow and keeping at this temperature for 2 h, (b) the same as (a) and then reducing in H_2 flow at 400 °C and (c) heating up to 500 °C in He flow and keeping at the latter temperature for 2 h. The heating rate was 2 °C min^{-1} for all of these treatments. The resulting catalysts were named ''gas treated catalysts'' (gas = He, O_2 or H_2) while those solids which had been under reaction for 10 h at 500 °C with 2% water added to the typical stream (see below) were denominated ''tested catalysts''. Table 1 shows the Co content of the prepared samples.

2.2. Bulk characterization

2.2.1. Temperature-programmed reduction (H_2-TPR)

These experiments were carried out with 0.05–0.10 g of either the fresh or the used catalyst using an Okhura TP-2002S instrument equipped with a TCD detector. Prior to the TPR measurements, the solids were pretreated in Ar heating up to 500 °C at 2 °C min^{-1}. The reducing gas was 5% H_2/Ar mixture. The flow rate was 30 cm^3 min^{-1}. The temperature was ramped up at a rate of 10 °C min^{-1} to 820–900 °C.

2.2.2. X-ray diffraction (XRD)

The XRD patterns of the fresh and used solids were obtained with an XD-D1 Shimadzu instrument operated at 35 kV and 40 mA. The scan rate was 1 ° min^{-1} for the 2θ range of 5–50°.

Table 1
Hydrogen consumption of the different Co, MOR treated in O_2

Catalyst	Co/Al	Co (wt.%)	H_2/Co peak I, T_I (°C)	H_2/Co peaks II + III, T_{III} (°C)	H_2/Co total
$Co_{8.85}$MOR	0.74	8.85	0.24 (327)	0.85 (848)	1.09
$Co_{5.70}$MOR	0.46	5.70	0.04 (390)	0.79 (820)	0.83
$Co_{2.91}$MOR	0.23	2.91	0.02 (400)	0.85 (900)	0.87
$Co_{2.45}$MOR	0.20	2.45	0	0.96 (830)	0.96
$Co_{1.15}$MOR	0.09	1.15	0	1.00 (950)	1.00

2.2.3. Raman spectroscopy

The Raman spectra were recorded with a TRS-600-SZ-P Jasco Laser Raman instrument, equipped with a CCD (change-coupled device) with the detector cooled to about −120 °C using liquid N_2. The excitation source was the 514.5 nm line of a spectra 9000 photometrics Ar ion laser. The laser power was set at 30 mW. Before the spectra were recorded the powder samples, fresh and used, were pressed at 4 bar into self-supporting wafers.

2.3. Surface characterization

2.3.1. Temperature-programmed NO desorption (NO-TPD)

The temperature-programmed NO desorption data were obtained using a continuous flow, fixed-bed and quartz microreactor operated under atmospheric pressure. In the reactor, 0.1 g of catalyst was treated following the methods described in Section 2.1. The reactor was cooled down to 25 °C and flushed with He for 15 min. The inlet flow was then switched to a 50 cm^3 min^{-1} flow of 1000 ppm NO/He mixture for 20 min. At the same temperature, pure He (50 cm^3 min^{-1}, 20 min.) was used to remove the gas-phase and reversibly adsorbed NO. The TPD experiment was carried out by heating up the sample at a rate of 5 °C min^{-1} while maintaining the He flow. The desorbed NO_x was monitored by a Fourier-transform infrared spectrometer (FTIR), Thermo Matson Genesis II, equipped with a gas 15-cm path-length IR cell.

2.3.2. NO adsorption: FTIR study

These experiments were carried out with the same spectrometer used for NO-TPD experiments. Finely powdered catalyst samples were pressed (6 tonnes, 5 min) into self-supporting wafers. Each wafer was inserted into a quartz sample holder with a furnace for the *in situ* activation of the sample. The sample holder was attached to the IR cell with F_2Ca windows. After the pretreatment program, it was allowed to cool to room temperature and the spectrum of the activated sample was collected. The adsorption procedure involved contacting the activated wafer with NO at RT for 15 min and outgassing with He to remove the NO gas-phase. Then, the temperature was increased in steps (100, 120, 150, 200 and 250 °C) and an FTIR spectrum at RT was collected after each step. The spectra of adsorbed NO species following each evacuation step were obtained by subtracting the spectrum of the activated wafer.

2.4. Catalytic test

Catalyst powders were tested in the same reactor described under NO-TPD experiments (Section 2.3). The typical composition of the reactant stream was the following: 1000 ppm CH_4, 1000 ppm NO and 2% O_2 in He (GHSV: 7500 h^{-1}). The composition of the reactor effluent was monitored for CH_4, CO, NO, N_2O and NO_2 using the FTIR described in Section 2.3. One hundred and fifty scans were collected with a nominal resolution of 1 cm^{-1} and averaged to get a spectrum. The CH_4 to CO_2 and the NO_x to N_2 conversions were defined as $C_{NO_x} = (1 - [NO_x]/[NO_x]^0) \times 100$, and $C_{CH_4} = (1 - [CH_4]/[CH_4]^0) \times 100$. $[NO_x]^0$ and $[CH_4]^0$ stand for the NO and CH_4 concentration of the feed, respectively. N_2 was measured by nitrogen balance.

3. Results

3.1. Temperature-programmed reduction (TPR)

In order to study the reducibility of Co sites in Co-exchanged NH_4–mordenite and to elucidate what kind of Co species were present on the samples, TPR experiments were performed. The TPR H_2 consumption and profiles are reported in Table 1 and Fig. 1, respectively. The incorporation of Co into the zeolitic matrix was done by ionic exchange. Even though all the catalysts were filtered and washed after the exchange procedure, cobalt oxides species could be formed due to hydrolysis of Co^{2+} [9]. This hydrolysis would be favored by the increasing cobalt loading concentration.

The $Co_{8.85}$MOR (Fig. 1A) reduction profile presents three peaks at 327, 680 and 850 °C. The first one is associated with Co oxide species like Co_3O_4 [6,9,10]. The second one is attributed to CoO_x and hydroxo-Co species [9,13]. The latter signal is assigned to Co^{2+} at exchange positions in the zeolitic matrix, which is more resistant to reduction because it is stabilized by the zeolite framework [4,6,9,10].

Samples with low Co loading ($Co_{2.45}$MOR and $Co_{1.15}$MOR) show a main peak at high temperatures meaning that almost all the Co cations are at exchange sites of the zeolitic matrix (Fig. 1D and E). The $Co_{2.91}$MOR TPR profile also shows two small peaks, one at 295 °C indicating the presence of a little amount of Co_3O_4, and the other at 505 °C attributed to CoO_x and hydroxo-Co species [9,13]. The peak at 390 °C in the $Co_{5.70}$MOR profile indicates that this sample contains oxide species and Co^{2+} at exchange position (Fig. 1B).

After being tested in a reaction feed with 2% water vapor for 10 h, some reorganization of cobalt species was expected to take place on the catalysts. The TPR results of the tested sample with 8.85 wt.% cobalt show that the H_2/Co ratio and the reduction temperature of peak I are almost identical to those observed for the O_2 treated solid (Table 2). However, the peak of the former (not shown) is sharper than the latter, probably because during the reaction the CoO_x particles tend to form a unique species having less interaction with the zeolite matrix. On the other hand, the H_2/Co ratio for peaks II and III notably decreases for the tested $Co_{8.85}$MOR (Table 2). This observable

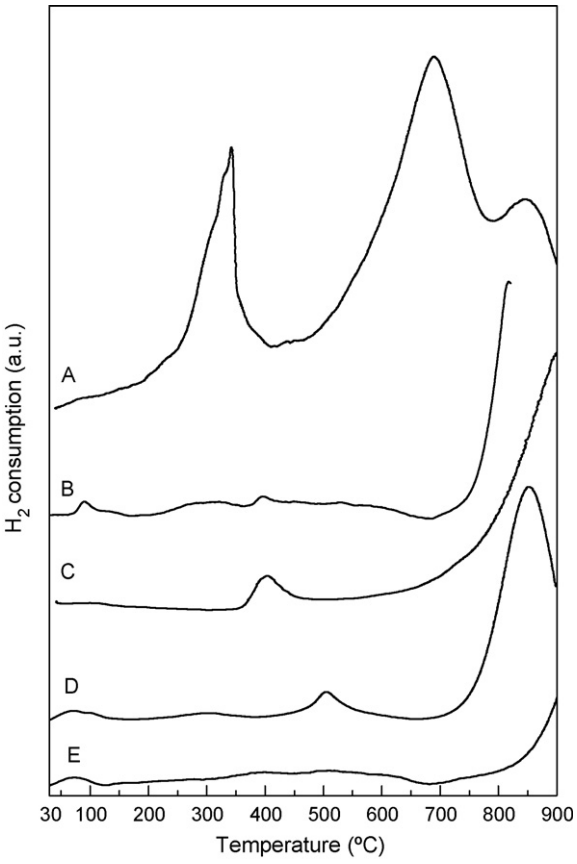

Fig. 1. TPR profiles of fresh samples treated in O_2. (A) $Co_{8.85}$MOR, (B) $Co_{5.70}$MOR (the TPR experiment was carried out up to 820 °C), (C) $Co_{2.91}$MOR, (D) $Co_{2.45}$MOR, and (E) $Co_{1.15}$MOR.

fact could be caused because some Co ions migrate to hidden exchange sites with highest coordination [12] and/or react with H_2O producing CoO_x particles.

The TPR results of the tested $Co_{1.15}$MOR catalyst indicate the formation of a small amount of Co_3O_4 during the reaction test (Table 2). Besides, the H_2/Co ratio also decreased as observed for the tested $Co_{8.85}$MOR (Table 2). These results would be indicative of the migration of exchanged Co to hidden exchange sites with higher coordination, which are hard to reduce [12].

3.2. NO adsorption and its temperature-programmed desorption (NO-TPD)

The NO adsorption capacity of these catalysts is also studied by NO-TPD experiments. Table 3 shows the results. All profiles

Table 2
Hydrogen consumption of calcined and tested samples

Catalyst	Treatment	H_2/Co peak I, T_I (°C)	H_2/Co peaks II + III, T_{III} (°C)	H_2/Co total
$Co_{8.85}$MOR	O_2	0.24 (327)	0.85 (848)	1.09
	Tested	0.24 (340)	0.63 (850)	0.87
$Co_{1.15}$MOR	O_2	0	1.00 (950)	1.00
	Tested	0.03 (268)	0.67 (950)	0.70

Table 3
NO adsorption

Pretreatment (T, °C)	$Co_{8.85}MOR$			$Co_{5.70}MOR$		$Co_{2.91}MOR$		$Co_{2.45}MOR$		$Co_{1.15}MOR$	
	NO/Co	NO_2/Co	N_2O/Co	NO/Co	NO_2/Co	NO/Co	NO_2/Co	NO/Co	NO_2/Co	NO/Co	NO_2/Co
He (500 °C)	0.55	0	0	0.60	0	0.71	0	1.20	0	1.25	0
H_2 (400 °C)	0.38	0	0.007	0.42	0	0.61	0	0.77	0	1.10	0
O_2 (500 °C)	0.55	0.016	0	0.62	0.35	0.80	0.096	1.30	0.13	1.70	0.35
H_2O (500 °C)	0.20	0.02[a], 0.06[a]	0	–	–	–	–	–	–	0.84	0.03[a], 0.16[a]

[a] NO desorption corresponding to two different peaks.

(not shown) seem to be very similar, with a maximum desorption temperature range between 120 and 150 °C; about 350 °C NO is completely desorbed. The NO/Co ratio decreases as the Co loading increases. The profiles of the samples pretreated in diluted O_2 flow show not only the NO desorption peak but also a small NO_2 one. This behavior may be due to the presence of some NO interaction with O_2 remaining in the zeolitic matrix. Besides, when NO is desorbed from the $Co_{8.85}MOR$ reduced sample, a small amount of N_2O is recorded, probably due to some surface reoxidation of Co^0.

$Co_{1.15}MOR$ has a NO/Co ratio close to 2. However, in the sample with 8.85 w% Co loading this ratio decreases to 0.55. This effect may be due to the presence of Co_xO_y agglomerations which decrease the amount of Co interacting with NO and/or may block up the zeolite channels. The NO/Co ratio obtained in the $Co_{5.7}MOR$ sample was lower than that in the $Co_{2.91}MOR$ but higher than that in $Co_{8.85}MOR$. This trend agrees with the Co oxide content of each sample.

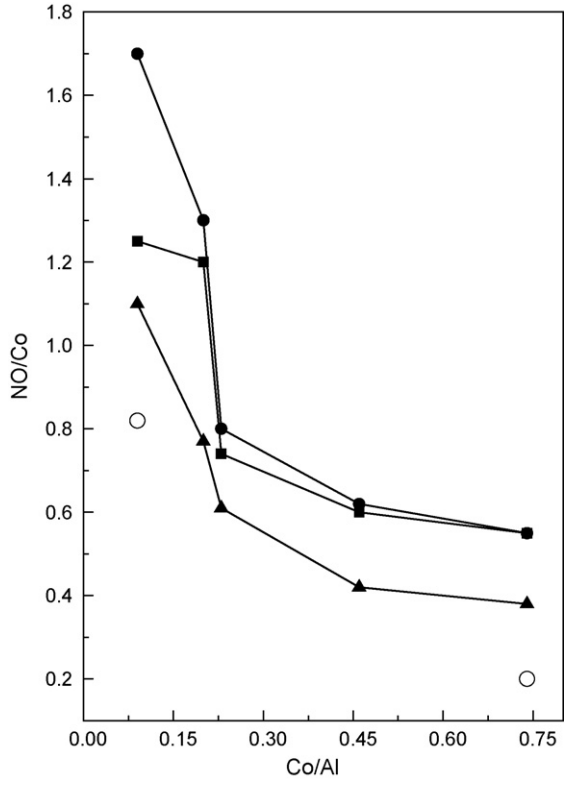

Fig. 2. NO adsorption results: Co/Al effect on the NO/Co ratio upon different pretreatments. (■) He, (▲) H_2, (●) O_2, and (○) tested catalysts.

In the samples with very similar Co loading ($Co_{2.91}MOR$ and $Co_{2.45}MOR$), a similar trend is observed for the NO/Co ratio. The former has some amount of Co_xO_y, and the NO/Co ratio results 0.8 whereas the latter, which is free of Co oxides, corresponds to a NO/Co ratio of 1.3. Therefore, the presence of Co_3O_4 again negatively affects the adsorption capacity.

For the NO-TPD of all samples pretreated with He, the NO adsorption capacities and the NO/Co ratios are lower than those obtained with the O_2 treatment, except for $Co_{8.85}MOR$ (Table 3). During the He treatment, the migration of cobalt species to inaccessible sites into the zeolitic structure would be taking place [5,10] but this effect is negligible in high Co loading samples. Additionally, during the He pretreatment a partial reduction of Co takes place as reported by Gutierrez et al. [12].

Fig. 2 shows the dependence of NO adsorption on the Co/Al ratio for the five samples after being heated in O_2, He, and H_2 atmospheres. The NO adsorption capacities of the samples with low Co loading strongly decrease when those solids are treated in He and H_2. However, catalysts containing some Co_xO_y, such as $Co_{2.91}MOR$, $Co_{5.7}MOR$ and $Co_{8.85}MOR$, present a similar adsorption capacity after treatments in He and O_2 atmospheres and a small decrease in the case of being treated in H_2. These results indicate that the adsorption depends not only on the location of exchanged Co but also on the presence of Co oxide which may block internal zeolite pores, thus hampering the exchanged Co^{2+} mobility to hidden sites.

The NO-TPD experiment of the tested catalysts was also performed (Table 3). The results reveal that the wet reaction feed negatively affects the NO adsorption capacity of both samples, $Co_{8.85}MOR$ and $Co_{1.15}MOR$. The NO/Co ratio decreased and the maximum peak temperature shifted toward lower temperatures (not shown). On the other hand, the NO_2/Co ratio increased in both samples and NO_2 desorption occurred at two different temperatures. This could be due to the oxidation of NO by some surface Co^{n+} or to some oxygen occluded in the zeolitic matrix during the reaction, or both as reported by Li and Armor [2].

3.3. Raman spectroscopy

Fig. 3A1 and A2 shows the Raman spectra of $Co_{8.85}MOR$, tested and O_2 treated samples. Both spectra are almost identical and the presence of the main signal of Co_3O_4 (680 cm^{-1}) is observed. This is in agreement with the TPR results which indicate that the amount of Co_3O_4 species remained the same after being tested in the wet reaction feed (Table 2).

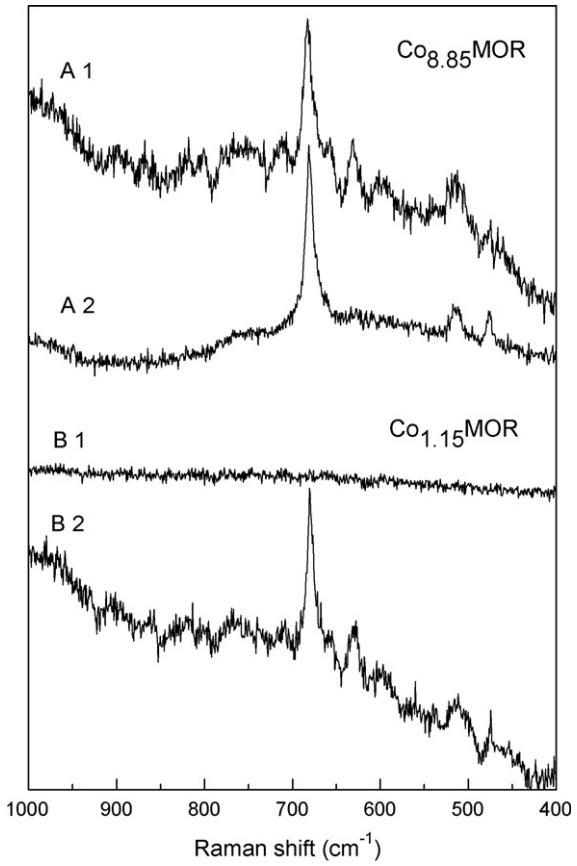

Fig. 3. Raman spectra of Co, mordenites. $Co_{8.85}$MOR: (A1) calcined and (A2) tested; $Co_{1.15}$MOR: (B1) calcined and (B2) tested.

The Raman spectrum of tested $Co_{1.15}$MOR shows the characteristic signal of Co spinel at 680 cm^{-1}, which is clearly absent from the spectrum of the one treated with O_2 (Compare with Fig. 3B1 and B2). These results were expected considering the TPR profiles of these catalysts.

3.4. Infrared spectroscopy: NO adsorption

3.4.1. The OH stretching region

The spectra of all prepared Co–MOR after the different pretreatments show the following features: (i) a peak centered at 3745 cm^{-1} assigned to the O–H stretching vibrations of terminal silanols, (ii) a broad band at 3600 cm^{-1} due to the OH stretching mode Si(OH)Al groups (Brønsted groups) and (iii) a shoulder at 3660 cm^{-1}, which could be associated with either $(Co–OH)^+$ species at exchange positions [9] or extraframework aluminum (EFAl) [15]. Taking into account that the latter signal (3660 cm^{-1}) was absent from the IR spectrum of the parent mordenite, the said signal would be attributed to hydroxo-cobalt ions in the O_2 and He treated catalysts.

In order to analyze the difference on the OH region of the IR spectra between catalysts treated with O_2 and those treated with wet reaction feed, the integrated absorbance ratios, I_{3740}/I_{1620} and I_{3660}/I_{1620}, were calculated; they are depicted on Table 4. I_{3740} and I_{3660} are the integrated absorbances of OH vibrations at 3740 and 3660 cm^{-1} and I_{1620}, integrated absorbance of T–O vibrations at 1620 cm^{-1}, characteristic signal of the mordenite structure, which was taken as reference. Both ratios, I_{3740}/I_{1620} and I_{3660}/I_{1620}, for the tested catalyst with 1.15% Co loading are somewhat higher than those treated with O_2 whereas for $Co_{8.85}$MOR, the difference between the I_{3740}/I_{1620} ratios of both treatments is more important suggesting that during the wet reaction test an increase of the sylanol group took place. This means that some dealumination occurred during this test generating sylanol species.

Table 4
Integrated absorbance ratios

Catalyst	Treatment	I_{3740}/I_{1620}	I_{3660}/I_{1620}
$Co_{1.15}$MOR	O_2	0.074	0.140
	Tested	0.078	0.157
$Co_{8.85}$MOR	O_2	0.062	0.250
	Tested	0.160	0.250

3.4.2. NO_{ads} vibration region

NO is a strong Lewis base and, when it has a σ-bonded interaction it is more firmly adsorbed on cationic sites. Besides, the presence of an unpaired electron in the molecule determines the trend of NO to adsorb as dimers [16].

In order to obtain some information about the adsorbed NO species and their interaction with the exchanged Co sites, the IR spectra of the catalyst after the adsorption of NO were obtained. Figs. 4–6 show the IR spectra of NO adsorbed on $Co_{1.15}$, $Co_{2.91}$ and $Co_{8.85}$MOR recorded at room temperature in flowing He.

Upon evacuation at different temperatures, the main bands at 1940, 1897 and 1814 cm^{-1} were monitored. The bands at 1814 and 1897 cm^{-1} were assigned to dinitrosyl species (Co^{2+}–$(NO)_2$) with 1814 cm^{-1} being the asymmetric stretching frequency, and 1897 cm^{-1} the symmetric stretching frequency. The signal at 1940 cm^{-1} indicates the presence of a mononitrosyl species adsorbed on a Co^{2+} ion at a specific exchange position [16].

Fig. 4 shows the spectra obtained for NO adsorption on $Co_{1.15}$MOR under the three different pretreatments. After evacuation at 25 °C, the three bands mentioned above are present and an additional shoulder at 1952 cm^{-1} is detected for the samples pretreated in He and O_2. This signal is assigned to mononitrosyl species adsorbed on Co^{2+} species with a different neighborhood. This adsorbed species seems to be unstable as it disappears at 150 °C.

When this solid is pretreated with He, mono- and dinitrosyl species disappear simultaneously with the temperature increase. The NO spectrum of the catalyst calcined with O_2 (Fig. 4B) shows the same adsorbed species but they seem to be more unstable as they disappear at 200 °C. At this temperature, NO_2 is produced as determined in the NO-TPD experiments. Then, the reaction of the adsorbed NO with the surface oxygen forming NO_2 can take place.

The reduced sample shows a very different behavior (Fig. 4C) as the mononitrosyl band is weak and disappears at 100 °C. The dimer species is stable up to 250 °C. The Co located at the exchangeable sites responsible for the mononitrosyl adsorption is

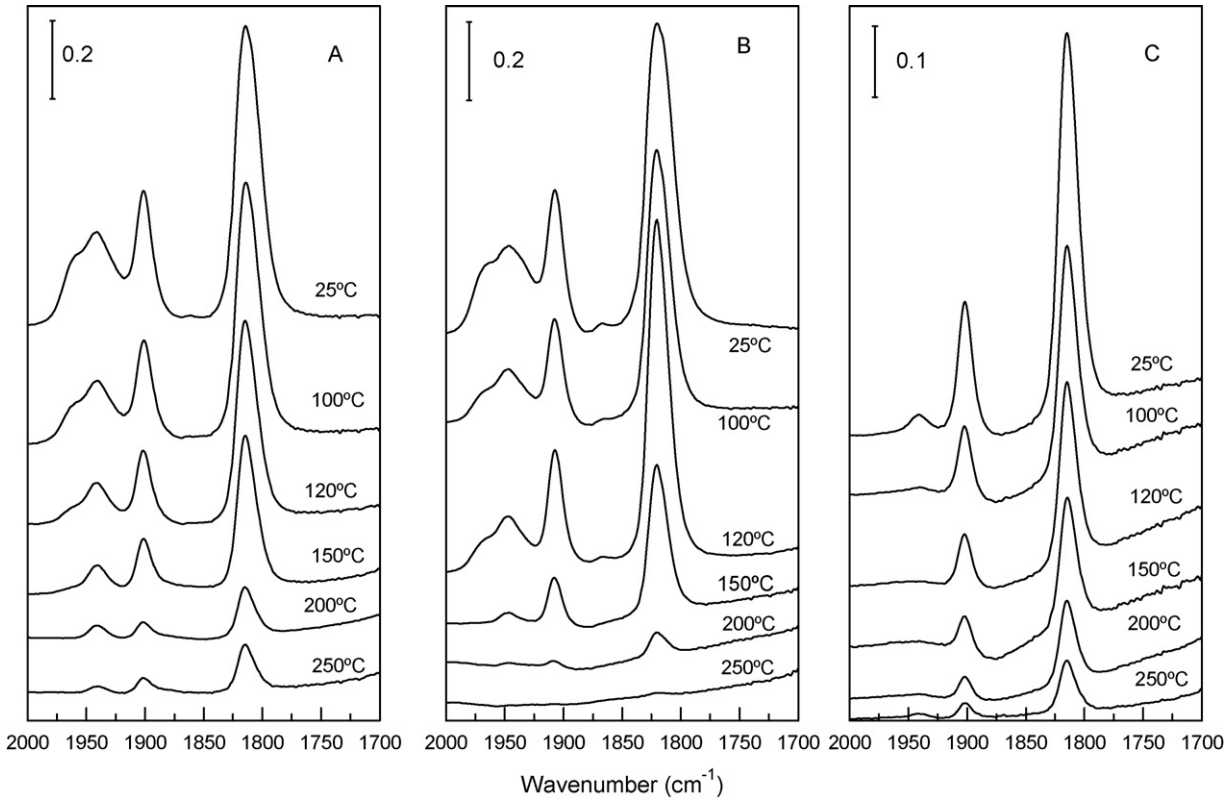

Fig. 4. IR spectra of NO adsorbed on $Co_{1.15}$MOR, at different temperatures recorded at room temperature. Pretreatment: (A) He, (B) O_2, and (C) H_2.

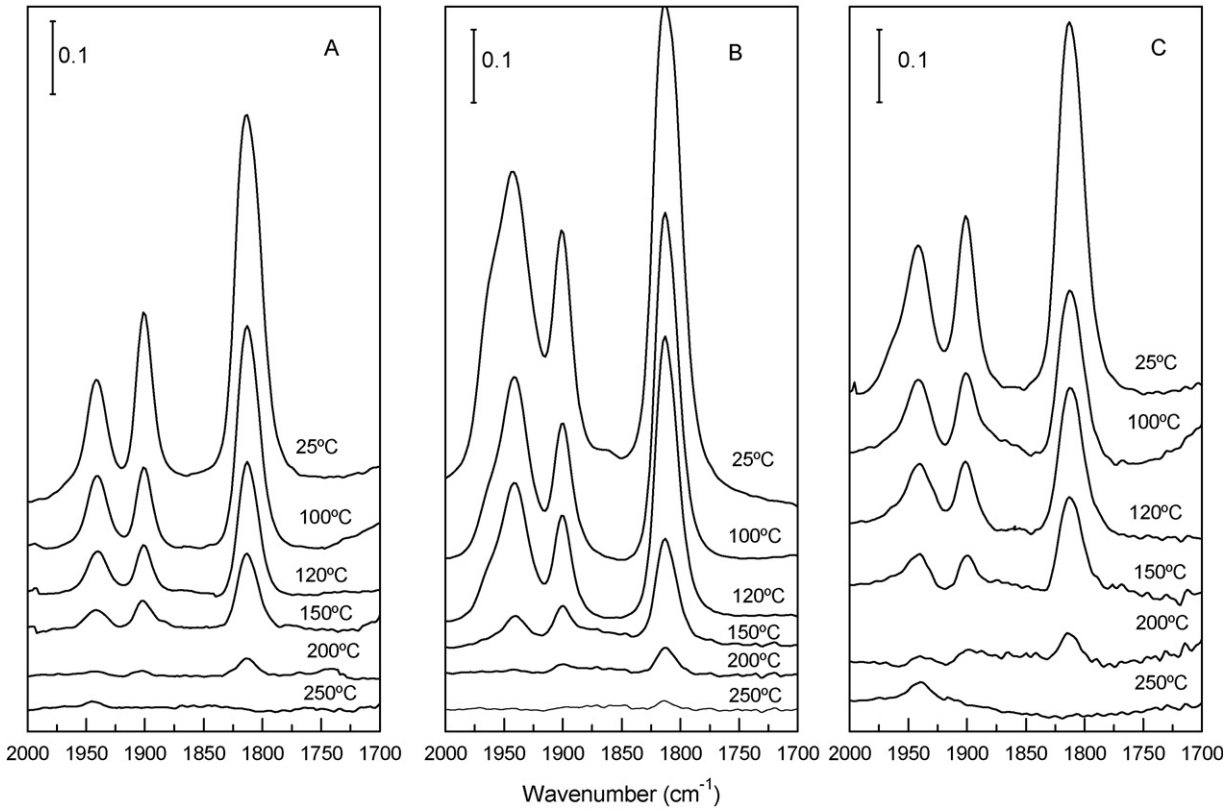

Fig. 5. IR spectra of NO adsorbed on $Co_{2.91}$MOR, at different temperatures recorded at room temperature. Pretreatment: (A) He, (B) O_2, and (C) H_2.

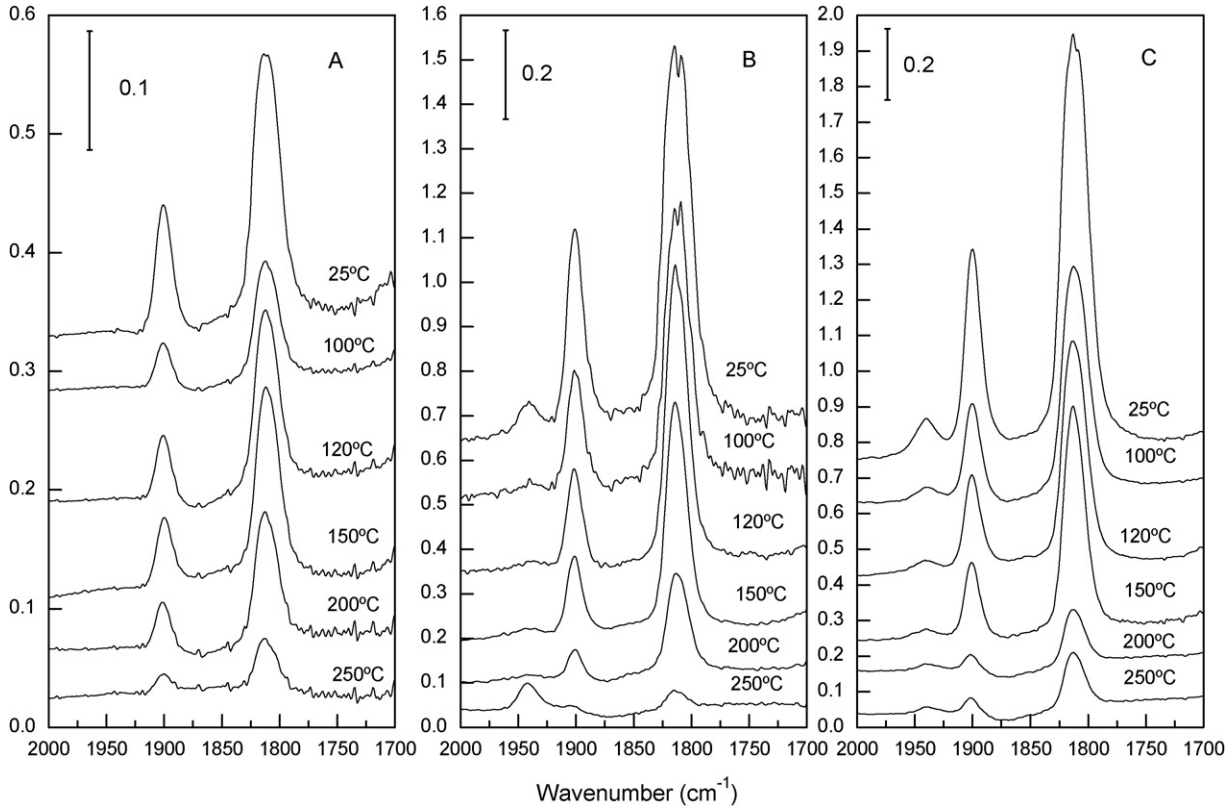

Fig. 6. IR spectra of NO adsorbed on $Co_{8.85}$MOR, at different temperatures recorded at room temperature. Pretreatment: (A) He, (B) O_2, and (C) H_2.

found to migrate to inaccessible sites of the zeolitic matrix during the H_2 pretreatment.

Fig. 5 shows the IR spectra of NO obtained for the $Co_{2.91}$MOR. The adsorbed NO species are similar to those of $Co_{1.15}$MOR, except that the monomer formed at 1940 cm^{-1} is more relevant. When this sample is treated with O_2 (Fig. 5B) the mononitrosyl is desorbed from the zeolitic surface simultaneously with the dinitrosyl species up to 200 °C. According to the NO-TPD results at this temperature, the formation of NO_2 takes place due to the reaction between the adsorbed NO and the surface oxygen.

To test the effect of oxide species over the surface NO adsorption, similar experiments were performed on the $Co_{8.85}$MOR catalyst. Fig. 6A–C shows the recorded IR spectra of adsorbed NO. At 25 °C, the dinitrosyl band is the dominant form of NO adsorbed on this sample for any treatment (Fig. 6A–C). These species remained adsorbed up to almost 250 °C. No mononitrosyl species were observed in this solid treated in He (Fig. 6A), although a very weak and unstable one was present in the sample treated in O_2 and H_2 (Fig. 6B and C).

The analyses of adsorbed NO species over the catalyst surfaces after being tested on wet reaction feed were also carried out and their IR spectra are shown in Fig. 7. Two mononitrosyl species at 1945 and 1925 cm^{-1} and dinitrosyl species (asymmetric and symmetric stretching frequencies at 1897 and 1810 cm^{-1}, respectively) were present on both tested samples, $Co_{8.85}$MOR and $Co_{1.15}$MOR (Fig. 7A and B, respectively). Even though the IR vibration frequencies of those species were the same as those observed on the fresh catalysts, the absorbance intensities of each species were remarkably different, mainly for the mononitrosyl one (compare Figs. 4B–7A and 6B–7B). Moreover, the stabilities with the increase of the desorption temperature for the mononitrosyl species on the tested catalysts were clearly higher, symptomatic of different adsorption sites. These new sites, probably CoO_x particles, were formed during the test reaction under wet conditions, most likely caused by the migration of Co species toward Co-free binding sites in the zeolite, as reported by Martínez-Hernández et al. for Co-ZSM5 [11].

3.5. Catalytic test

The results of the catalytic activity tests are reported in Table 5. In all the tests, the products are NO_2, N_2 and CO_2. Neither CO nor N_2O are detected. The lowest NO to N_2 conversion occurs with $Co_{8.85}$MOR, because of the presence of non-desired Co_3O_4, as it only promotes the oxidation of methane with oxygen instead of NO [10,12,14]. However, the best NO to N_2 conversion is shown by the 2.45 and 2.91 Co content samples, in agreement with Li and Armor [1,3] who reported that there is an optimum amount of Co^{2+} in the zeolitic structure which makes the catalyst highly active to the SCR with methane.

$Co_{8.85}$MOR and $Co_{1.15}$MOR were tested in the wet reaction feed at 500 °C for 10 h and their catalytic results are shown in Table 5. $Co_{8.85}$MOR resulted inactive for NO reduction after the ‘‘tested’’ treatment; however, methane was completely

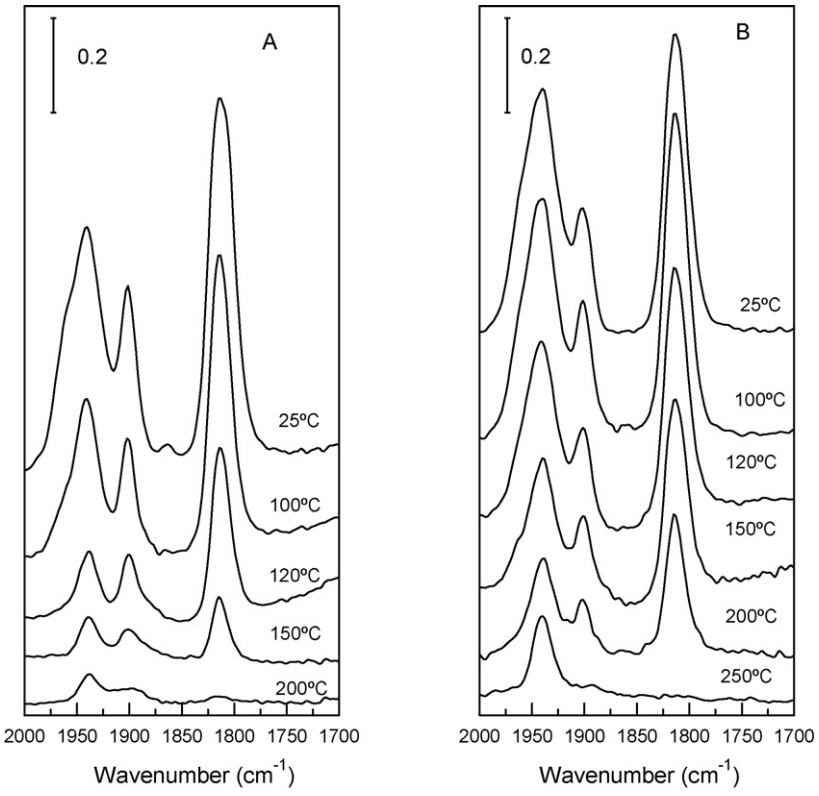

Fig. 7. IR spectra of NO adsorbed on (A) $Co_{1.15}$MOR and (B) $Co_{8.85}$MOR, at different temperatures recorded at room temperature. These catalysts were tested in wet reaction feed at 500 °C for 10 h.

Table 5
Catalytic data[a]

Catalysts	Pretreatment	Reaction temperature (°C)					
		450		500		550	
		C_{NO} (%)	C_{CH_4} (%)	C_{NO}	C_{CH_4} (%)	C_{NO} (%)	C_{CH_4} (%)
$Co_{8.85}$MOR	O_2	16	97	5	100	2	100
	Tested	0	100	1	100	0	100
$Co_{5.70}$MOR	O_2	40	60	29	90	20	100
$Co_{2.91}$MOR	O_2	46	98	30	100	10	100
$Co_{2.45}$MOR	O_2	47	80	35	100	21	100
$Co_{1.15}$MOR	O_2	37	48	33	88	8	100
	Tested	33	42	29	80	7	99

[a] Catalytic activity measurements performed under dry conditions.

consumed. This behavior suggests that a significant amount of active species for the NO reduction were transformed into Co oxide entities. On the $Co_{1.15}$MOR solid both the NO and CH_4 conversion dropped simultaneously.

4. Discussion

4.1. Effect of the pretreatments and the Co content on exchange sites

NO strongly adsorbs on cationic sites and the mordenite structure presents three types of exchanged Co^{2+} denoted as α, β and γ [17]. The α-type Co ions are located in the main channel of the zeolitic structure and have a weak bonding to the framework oxygen. These two features present the α-Co site with a high tendency to form dinitrosyl species under NO adsorption. The β-type Co ions are placed in the interconnected small channel of the mordenite and have medium strength bonding to framework oxygen with a high ability to adsorb mononitrosyl. The γ-type Co ions are in the ''boat-shaped'' sites and are the most highly coordinated cation sites in the mordenite. Therefore, they are expected to offer no contribution to the NO adsorption. The order to the strength bond of the Co ions to the framework is α < β < γ-type Co. So the NO adsorption capacity on the Co ions follows the reverse order [17].

The $Co_{1.15}$MOR sample treated in either He or O_2 would mostly have the exchanged Co in α and β sites responsible for dinitrosyl and mononitrosyl adsorptions, respectively. Moreover, the two mononitrosyl bands observed in the IR spectra (Fig. 4A and B) would indicate the presence of two slightly different β sites. On the other hand, when this sample is treated in H_2 at 350 °C, the mononitrosyl bands notably decrease (Fig. 4C). This fact suggests that a significant amount of β-type Co ions migrate to inaccessible sites such as γ. The Co placed on this γ-type site would adsorb a negligible amount of NO, the NO/Co ratio decreasing as seen in Table 3.

However, when $Co_{2.91}$MOR is treated in He, the NO adsorbed as dinitrosyl form is the main signal and there is a contribution of the mononitrosyl species at 1940 cm^{-1} (Fig. 5A). Both NO species desorbed at the same temperature.

Similar results were obtained on the reduced catalyst (Fig. 5C). Then, both treatments, in He and H_2, would induce the migration of exchanged Co in α and β sites to inaccessible sites, this effect being more severe on the exchanged Co responsible for mononitrosyl adsorption (β site).

Comparing NO IR spectra of $Co_{1.15}$MOR and $Co_{2.91}$MOR treated in O_2 (Figs. 4B and 5B), the mononitrosyl species at 1940 cm^{-1} (β site) and the dinitrosyl species (α site) are more significant for the latter sample, suggesting that as the Co loading increases the Co cations are mostly exchanged in these two kinds of sites.

The $Co_{8.85}$MOR contains Co_3O_4 according with the TPR profile and Raman spectra (Figs. 1A and 3A1) but the particle sizes are small enough no to be detected by XRD. Besides, the NO adsorbed as mononitrosyl in this particular sample is negligible suggesting that the small clusters of Co_3O_4 would essentially block the access of NO to some β sites whereas the accessibility of the α sites in the main channel of mordenite would be unaffected by the spinel. This blocking effect is also supported by the fact that no significant changes are observed on the NO adsorption capacities of this sample after the three different treatments (Table 3). During the pretreatment in He or H_2, the migration of Co cations to inaccessible sites into the mordenite structure would be blocked by the Co oxide clusters. Another significant characteristic observed in this particular catalyst when treated in O_2 or H_2 (Fig. 6B and C) was the decrease of the dinitrosyl signal at 250 °C and the simultaneous growth of the band at 1940 cm^{-1}. This effect is associated with mononitrosyl species, indicating that the dimer acts as a precursor of the monomer. Besides, in the case of the sample treated in O_2, this behavior could also be explained considering that one NO of the dimer species adsorbed on oxo-Co particles ($O\text{-}Co(NO)_2$) reacts with the surface oxygen at high temperatures to produce NO_2, while the other NO adsorbed remains on the site.

The catalytic behavior of $Co_{8.85}$MOR after being in wet reaction at 550 °C for 10 h pointed out a significant drop of the active sites for NO reduction to N_2 since the NO conversion was almost negligible (Table 5). However, the methane conversion was complete meaning that all the hydrocarbon reacted with O_2, the presence of CoO_x particles favoring the latter reaction [10]. The formation of these CoO_x particles having less interaction with the zeolite matrix would take place during the reaction in the presence of H_2O [11]. The existence of these cobalt oxide agglomerates is also sustained by the NO_x-TPD results. A new NO_2 desorption peak at low temperature is observed which would be associated with the oxidation of adsorbed NO for surface Co^{n+} oxides. The reduction temperature of these cobalt species is attributed to peak I (Table 2). Even though there are no changes in these hydrogen consumption amounts for fresh and tested $Co_{8.85}$MOR, the characteristics of CoO_x agglomerates in fresh and tested samples are different. On the other hand, the total H_2/Co decreased in comparison to that of the fresh catalyst, suggesting that the migration of some Co^{2+} ions to hidden exchange sites with higher coordination also occurred, as reported by Gutierrez et al. [12].

In the case of the tested $Co_{1.15}$MOR, these new CoO_x particles were also formed during the test reaction under wet conditions as the TPR and NO_x-TPD results substantiated (Tables 2 and 3). However, the amount of those particles was smaller than that of the high Co-content sample since no significant changes on the CH_4 conversion were observed but only some decrease of the NO conversion (Table 5). Therefore, the formation of these Co oxide species in wet reaction stream would be favored by the Co ion closeness in the zeolite structure.

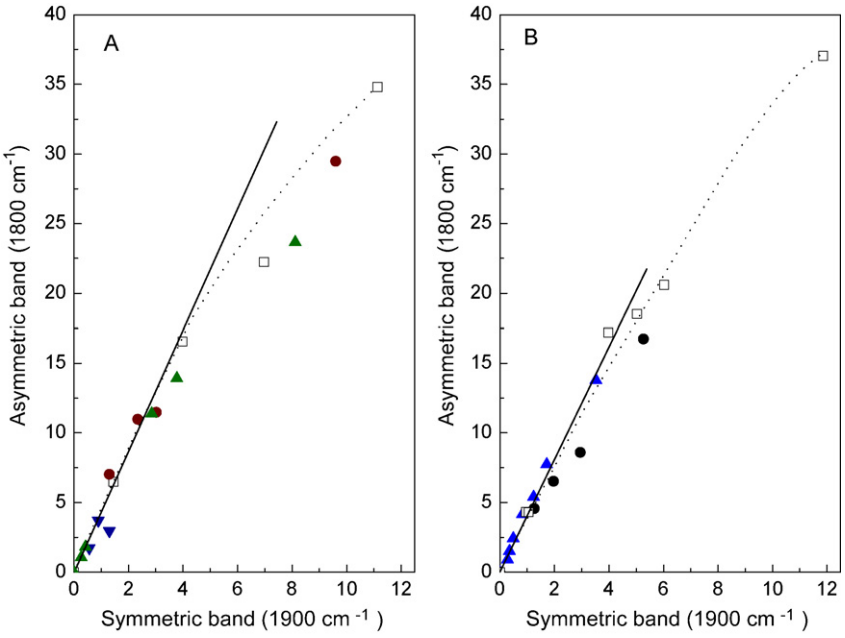

Fig. 8. Correlation of dinitrosyl symmetric and asymmetric bands. (□) $Co_{8.85}$MOR, (▲) $Co_{2.91}$MOR, (▼) $Co_{2.45}$MOR, (■) $Co_{1.15}$MOR, and (●) $Co_{5.70}$MOR. Pretreatment in: (A) O_2 and (B) H_2.

4.2. Nature of dinitrosyl species

The dominant NO species adsorbed on gas-treated Co_xMOR is found to be in dinitrosyl form since it is well known that the dihedral angles between the NO molecules of these species adsorbed on cobalt cations are small in order to avoid steric hindrance [18,19]. Moreover, the existence of two different Co sites of the dinitrosyl adsorption (α site) is inferred from Fig. 6B since two overlapping asymmetric vibrational bands around 1815 cm^{-1} are identified. Those sites are likely to be exchangeable sites IV and VI (nomenclature from [20]) located at the main channel on the mordenite structure where both sites have enough room for the dinitrosyls to form.

To explore the presence of these two dinitrosyl species for all the prepared Co–MOR and taking into account that the dihedral angle of the dinitrosyl species can be calculated from the ratio of the integrated intensities [20]:

$$\frac{I_{asym}}{I_{sym}} = \tan^2(\theta)$$

The integrated intensities of the asymmetric (I_{asym}) and symmetric (I_{sym}) stretching modes of dinitrosyl species were measured for the IR spectral studies here reported. The correspondence between I_{asym} and I_{sym} is shown in Fig. 8 and a non-linear correlation is observed which confirms that two distinctive dinitrosyl species are present despite the differences in Co loading. This evidence suggests that the part of exchanged Co cations located in sites IV and VI (α site) is present in all the samples and has the same characteristics. Moreover, one of these dinitrosyl species seems to be more stable at high temperatures having a dihedral angle of 123°.

5. Conclusions

The NO adsorption capacity and its relationship with the activity on Co–MOR have been studied for samples with different amounts of cobalt and different pretreatments: He heating, O_2 calcination, and H_2 reduction. The main features observed are the following:

- The presence of such oxides blocks some channels of the mordenite. The NO/Co ratio is lower than 1 because either the total Co ions are not accessible to the NO molecule to be adsorbed, or probably some Co island is formed on the zeolite surface, lowering the amount of surface Co (Table 3).
- Mono- and dinitrosyl are the main adsorbed species observed by FTIR and their stability and relative amount strongly depend on the pretreatments and cobalt species (Figs. 4–6).
- Heating in He or H_2 induces the stabilization of part of exchanged Co in less accessible gas-sites (γ-Co), whereas the calcination with O_2 involves the mobilization of some Co to more external sites (α- and β-Co). However, this effect is less significant for samples containing Co oxides, suggesting that the spinel hinders the Co migration to less accessible sites.
- For all samples, the α-Co sites would be located in sites IV and VI. One of these sites desorbs $(NO)_2$ dinitrosyl at higher temperature.
- Co_3O_4 negatively affects the NO to N_2 conversion, reducibility and the NO adsorption capacity for all pretreatments (Figs. 1–3; Tables 1–3 and 5).
- The formation of CoO_x agglomerates having less interaction with the zeolite matrix would take place during the reaction in the presence of H_2O and this process would be favored by the Co ion closeness in the zeolite structure. However, some Co^{2+} ions would also migrate to hidden exchange sites with higher coordination.

Acknowledgments

The authors wish to acknowledge the financial support received from UNL, CONICET and ANPCyT. They are also grateful to the Japan International Cooperation Agency (JICA) for the donation of the major instruments used in this study. Thanks are given to Elsa Grimaldi for the English language editing and to Andrea Feser and Juan Pablo Bortolozzi for their technical assistance.

References

[1] Y. Li, J.N. Armor, Appl. Catal. B 2 (1993) 239.
[2] Y. Li, J.N. Armor, J. Catal. 150 (1994) 376.
[3] J.N. Armor, Catal. Today 26 (1995) 147.
[4] L. Gutierrez, A. Boix, J.O. Petunchi, J. Catal. 179 (1998) 179.
[5] D. Kaucký, A. Vondrová, J. Dědeček, B. Wichterlova, J. Catal. 194 (2000) 318.
[6] C. Resini, T. Montanari, L. Nappi, G. Bagnasco, M. Turco, G. Busca, F. Bregani, M. Notaro, G. Rocchini, J. Catal. 214 (2003) 179.
[7] J. Dědeček, B. Wichterlova, J. Phys. Chem. B 103 (1999) 1462.
[8] J. Dědeček, D. Kaucký, B. Wichterlova, Micropor. Mesopor. Mater. 35/36 (2000) 483.
[9] M.A. Ulla, L. Gutierrez, E.A. Lombardo, F. Lónyi, J. Valyon, Appl. Catal. A 277 (2004) 227.
[10] A. Boix, E.E. Miró, E.A. Lombardo, M.A. Bañares, R. Mariscal, J.L.G. Fierro, J. Catal. 217 (2003) 186.
[11] A. Martínez-Hernández, G.A. Fuentes, Appl. Catal. B 57 (2005) 167.
[12] L. Gutierrez, M.A. Ulla, E.A. Lombardo, A. Kovács, F. Lonyi, J. Valyon, Appl. Catal. A 292 (2005) 154.
[13] F. Bustamante, F. Córdoba, M. Yates, C.M. De Correa, Appl. Catal. A 234 (2002) 127.
[14] M.C. Campa, S. De Rossi, G. Ferraris, V. Indovina, Appl. Catal. B 9 (1996) 315.
[15] T. Montanari, O. Marie, M. Daturi, G. Busca, Catal. Today 110 (2005) 339.
[16] K. Hadjiivanov, B. Tsyntsarski, T. Nikolova, Phys. Chem. Chem. Phys. 1 (1999) 4521.
[17] Z. Sobalík, J. Dědeček, D. Kaucký, B. Wichterlova, L. Drozdová, R. Prins, J. Catal. 194 (2000) 330.
[18] W. Zhang, Y. Yahiro, J.H. Izumi, M. Iwamoto, J. Chem. Soc., Faraday Trans. 91 (4) (1995) 767.
[19] L. Aparicio, J. Dumesic, S. Fang, M. Long, M.A. Ulla, W. Millman, K. Hall, J. Catal. 108 (1987) 233.
[20] W. Mortier, J. Phys. Chem. 81 (1977) 1334.